Available online at www.sciencedirect.com
ScienceDirect
International Journal of Heat and Mass Transfer 50 (2007) 857–871
International Journal of HEAT and MASS TRANSFER
www.elsevier.com/locate/ijhmt

Transient flow patterns and bubble slug lengths in parallel microchannels with oxygen gas bubbles produced by catalytic chemical reactions

Jinliang Xu *, Yi Feng, Jiwen Cen

Micro Energy System Laboratory, Guangzhou Institute of Energy Conversion, Chinese Academy of Science, Nengyuan Road, Wushan, Guangzhou 510640, PR China

Received 16 February 2006; received in revised form 17 August 2006
Available online 19 October 2006

Abstract

Transient flow patterns and bubble slug lengths were investigated with oxygen gas (O_2) bubbles produced by catalytic chemical reactions using a high speed camera bonded with a microscope. The microreactor consists of an inlet liquid plenum, nine parallel rectangular microchannels followed by a micronozzle, using the MEMS fabrication technique. The etched surface was deposited by the thin platinum film, which is acted as the catalyst. Experiments were performed with the inlet mass concentration of the hydrogen peroxide from 50% to 90% and the pressure drop across the silicon chip from 2.5 to 20.0 kPa. The silicon chip is directly exposed in the environment thus the heat released via the catalytic chemical reactions is dissipated into the environment and the experiment was performed at the room temperature level. It is found that the two-phase flow with the catalytic chemical reactions display the cyclic behavior. A full cycle consists of a short fresh liquid refilling stage, a liquid decomposition stage followed by the bubble slug flow stage. At the beginning of the bubble slug flow stage, the liquid slug number reaches maximum, while at the end of the bubble slug flow stage the liquid slugs are quickly flushed out of the microchannels. Two or three large bubbles are observed in the inlet liquid plenum, affecting the two-phase distributions in microchannels. The bubble slug lengths, cycle periods as well as the mass flow rates are analyzed with different mass concentrations of hydrogen peroxide and pressure drops. The bubble slug length is helpful for the selection of the future microreactor length ensuring the complete hydrogen peroxide decomposition. Future studies on the temperature effect on the transient two-phase flow with chemical reactions are recommended.

Keywords: Flow patterns; Microchannel reactor; Hydrogen peroxide; Bubble slug length; Liquid slug; Microthruster

1. Introduction

Microthrusters can provide the miniature thrust force in the order of micro-Newtons for the attitude control of nano-satellites with the weight of 10–100 kg. Thus they have been received great attention in recent years. Three types of microthrusters can be classified: cold gas [1], solid [2] and liquid propellant microthrusters [3].

In a liquid propellant microthruster, liquid such as water can be evaporated in a microchamber by the electric heating to produce vapor, which is being discharged through a micronozzle to acquire the thrust force [3].

Alternatively, the liquid hydrogen peroxide (H_2O_2) can be used in a microthruster. In such a microsystem, hydrogen peroxide can be self-decomposed via the catalytic chemical reactions to create the mixture of oxygen gas and water vapor for the thrust force applications [4]. Compared with the water microthruster, the hydrogen peroxide microthruster is an energy saving one without additional electricity needed, thus it has the potential applications in nano-satellites which are being developed.

Before the hydrogen peroxide microthrusters can be put into operation, a lot of issues should be overcome. The

* Corresponding author. Tel./fax: +86 20 87057656.
E-mail address: xujl@ms.giec.ac.cn (J. Xu).

0017-9310/$ - see front matter © 2006 Elsevier Ltd. All rights reserved.
doi:10.1016/j.ijheatmasstransfer.2006.08.017

Nomenclature

c	Moore concentration of the potassium permanganate solution, mol/L	m_{sam}	sample liquid mass of the hydrogen peroxide, g
c_1	inlet mass concentration of hydrogen peroxide	m	mass flow rate, g/s or kg/s
c_2	outlet mass concentration of hydrogen peroxide	V	the consumed volume of the potassium permanganate solution, ml
$c_{pf,water}$	specific heat of water, J/mol K or J/kg K	α	the decomposition ratio of the hydrogen peroxide after the microchannel reactor
c_{pv,O_2}	specific heat of oxygen gas, J/mol K or J/kg K	ΔP	pressure drop across the silicon chip, kPa
$c_{pv,water}$	specific heat of water vapor, J/mol K or J/kg K		
h_{fg}	latent heat of evaporation, J/mol or J/kg		

detailed review is beyond the scope of the present paper but can be found in a recent review article by Hitt et al. [4]. One of the important issues is to develop the method that ensures the complete decomposition of the liquid hydrogen peroxide. If the hydrogen peroxide is not decomposed completely in microreactors, liquid droplets occur and are flushed out of the microreactors, deteriorating the microthruster performance.

The liquid droplet formation in microreactors is strongly related to flow patterns with the catalytic chemical reactions. Two-phase flow patterns without chemical reactions were widely investigated in microchannels for the development of compact microchannel heat sinks. Kawajim and Chung [5] gave a review on the adiabatic two-phase flow in mini/microchannels. Channel size effect on the two-phase flow was performed by decreasing the hydraulic diameter of the microchannels. Only slug flow was observed and a new correlation was developed for the void fractions. The transition boundaries on the two-phase flow regime maps were shifted for the slug flow subcategories. Qu et al. [6] conducted experiments with adiabatic nitrogen–water two-phase flow in a rectangular microchannel having a $0.406 \times 2.032\ mm^2$ cross-section. The results reveal the dominant flow patterns are slug and annular flows with bubbly flow occurring occasionally. Flow patterns in mini/microchannels were also reported by Yun and Kim [7], Satichaicharoen and Wongwises [8].

Wu and Cheng [9] performed experiments with water as the working fluid in horizontal silicon microchannels. Various modes of boiling instabilities occur after the boiling incipience. An unsteady liquid/two-phase/vapor alternative flow was observed with large oscillation amplitudes and long cycle periods of the pressure drops and wall surface temperatures. Recently, Xu et al. [10] measured the transient flow patterns and heat transfer behavior in 10 silicon microchannels. The transient flow patterns were repeated in a timescale of millisecond. A cycle consists of three substages: liquid refilling stage, bubble nucleation, growth and coalescence stage and transient annular flow stage. Bubble explosion was observed after the coalescence of the isolated bubbles and pushed the fluid out of microchannels quickly. It is noted that fewer studies deal with the two-phase flow patterns with chemical reactions in microchannels. Fu and Pan [11] dealt with the two-phase flow in a single rectangular microchannel with CO_2 bubbles generated by chemical reactions of sulfuric acid (H_2SO_4) and sodium bicarbonate ($NaHCO_3$). The objective of such a study is for the removal of CO_2 bubbles for the design of a micro direct methanol fuel cell (DMFC). Bewer et al. [12] presented a method in situ production of bubbles in a test cell made of perspex. The method is to perform the hydrogen peroxide decomposition to oxygen gas and water in aqueous media at the presence of a catalyst. The oxygen gas generation rate is similar to the same order of magnitude as in real direct methanol fuel cells (DMFC).

The objective of the present study is to provide the high speed flow visualization on the transient flow patterns in a microchannel reactor. It is found that the isolated bubbles and bubble slugs are the dominant flow patterns. The flow patterns display the strong cyclic behavior, consisting of two critical times. One is at the beginning of the bubble slug flow stage on which the number of liquid slugs is maximum. The other is at the end of the bubble slug flow stage on which the number of liquid slugs is minimum and the fluid is quickly flushed out of the microchannels. The large bubbles are also observed in the inlet liquid plenum, affecting the two-phase distributions in microchannels. The bubble slugs are non-uniformly distributed in microchannels and have lengths shorter than the simple empirical catalyst lengths reported in aerospace for the macroscale HTP thrusters and scaled those predictions in MEMS scale. The present study provides the guideline for the selection of the future microchannel reactor length, ensuring the complete decomposition of the liquid hydrogen peroxide. The present experimental findings are also useful for the development of bio-chips using oxygen gas by chemical reactions [13].

2. Experimental detail

2.1. Design and fabrication of the microreactor

Fig. 1 shows the three-dimensional drawing of the microreactor chip, consisting of the etched silicon substrate bonded with a Pyrex glass. An inlet liquid plenum, nine parallel rectangular microchannels and a converging–diverging nozzle are etched in the silicon substrate, with the entire dimensions of $13485 \times 5120 \times 530\ \mu m^3$.

The inlet liquid plenum is a rectangular chamber with the width of 2.0 mm and length of 4.0 mm. The microchannel has the length of 6.0 mm, width of 80 μm and depth of 120 μm. The total width of the nine microchannels is 1120 μm. Because the fluid out of the silicon chip is directly discharged to the environment, the micronozzle followed by the microchannels is used to maintain higher pressures in microchannels. In the present paper, we focus on the hydrogen peroxide decomposition and two-phase flow in microchannels and inlet liquid plenum. A one-dimensional coordinate system was established at each rectangular microchannel centerline with the original point started from the microchannel entrance with the positive x as the flow direction.

Fig. 2 shows the chip fabrication process. Initially a n-type $\langle 100 \rangle$ silicon substrate is cleaned by the standard RCA procedure to remove the contamination on the chip surface (Fig. 2a). A 3 μm photoresist was deposited by spin coating on the clean polished surface (Fig. 2b). The exposed photoresist is developed after the photoresist was patterned by exposure to UV light through a designed mask (Fig. 2c). The deep inductively coupled plasma (ICP) etching was performed on the silicon wafer with the pattern transferred through photolithography. A

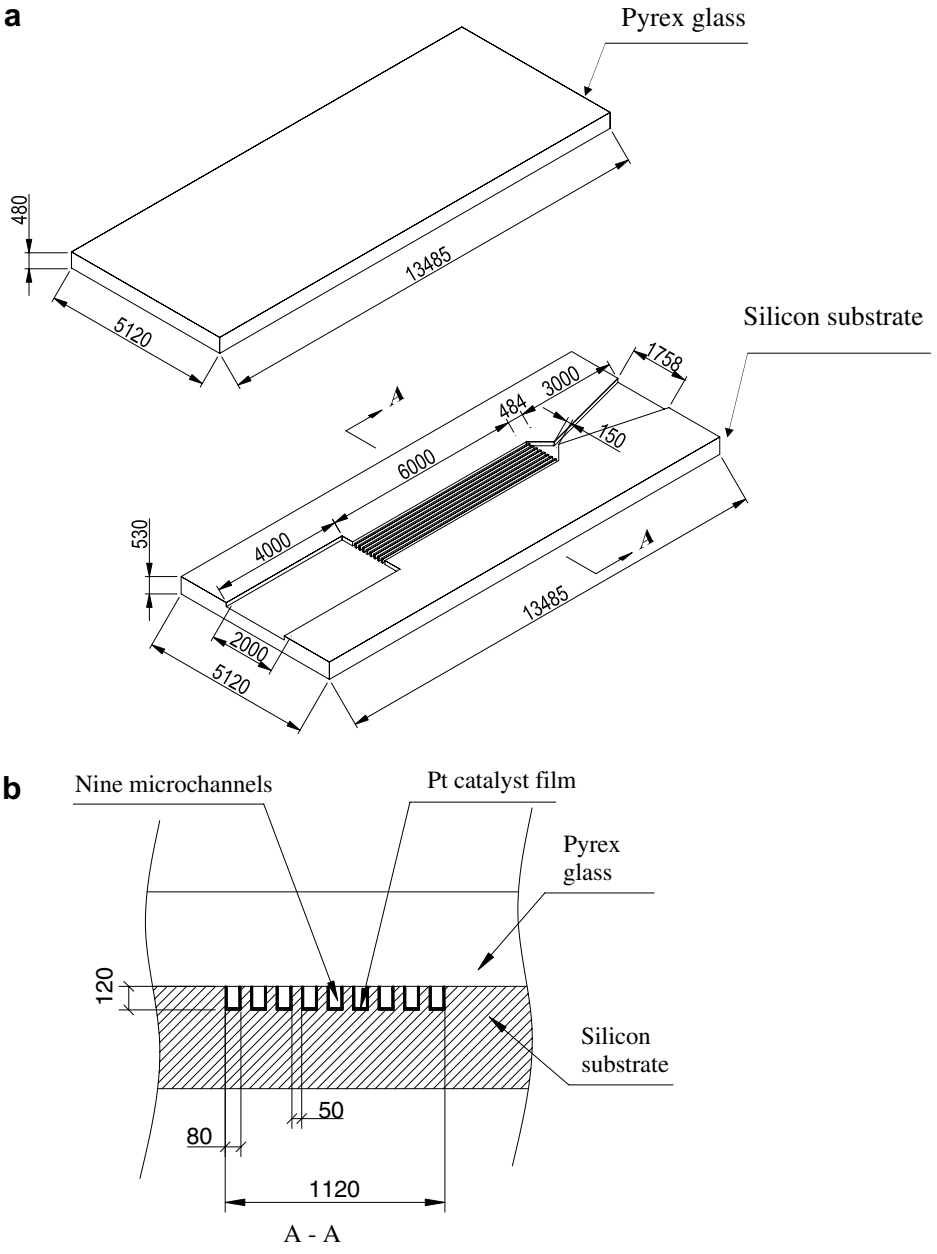

Fig. 1. Microchannel reactor including an inlet liquid plenum, nine parallel microchannels and a planar converging–diverging nozzle (all dimensions are in μm).

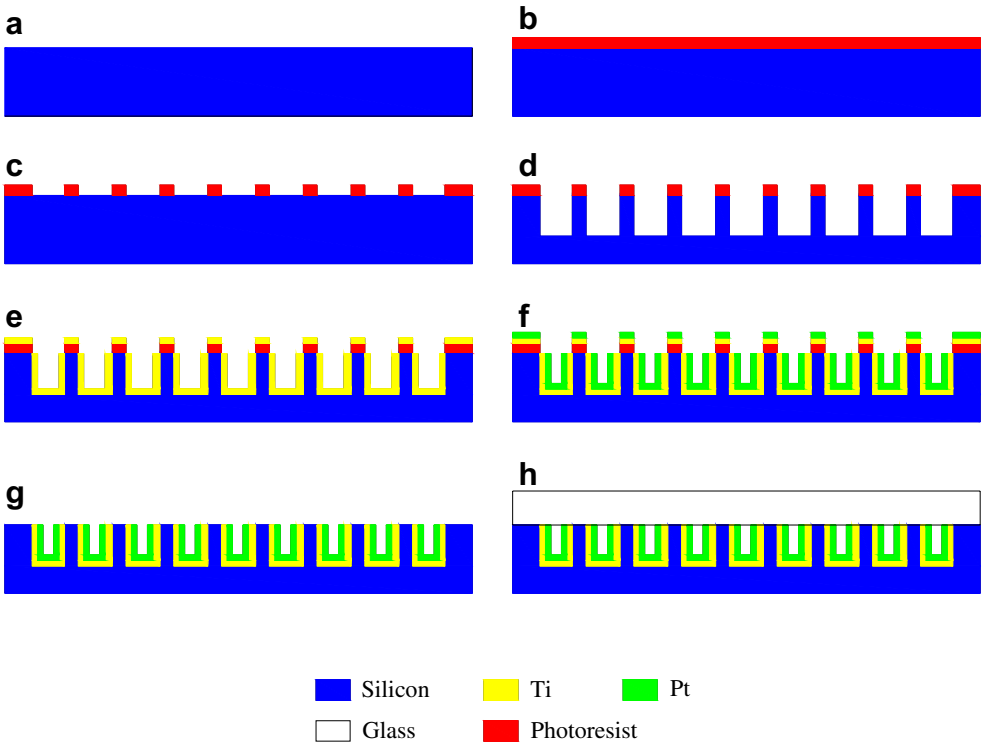

Fig. 2. The fabrication process of the silicon chip.

successive of SF_6 etch cycles and C_4F_8 passivation are included in the ICP process (Fig. 2d).

A polymer layer may be created on the silicon substrate during the ICP etching process, which will affect the adhesion performance between the silicon surface and the titanium film. Therefore, the polymer layer must be removed. The oxygen plasma treatment process was performed to clean such polymer layer. After such clean procedure, the titanium film of 400 Å (Fig. 2e) and platinum film of 1500 Å (Fig. 2f) were deposited successively. Then all the photoresist was removed by the dry striping process, with the oxygen plasma bombardmenting the wafer (Fig. 2g). The bonding process involves the connections of the silicon wafer with the anode electrode and the Pyrex glass with the negative electrode. After the whole chip is heated up to 350 °C, the 500 V voltage was applied to fulfill the bonding process (Fig. 2h). Finally, the chips were diced from the whole wafer to form pieces of individual microreactor chip.

2.2. Experimental setup

Fig. 3 shows the experimental setup. A high pressure nitrogen gas bottle is the pressure source to power the liquid hydrogen peroxide in its container to the silicon chip. The liquid phase is the mixture of the deionized water and pure hydrogen peroxide. A high precision pressure regulator is arranged in the pipeline between the nitrogen gas bottle and the liquid container to adjust the pressure at a required value. Because the high concentration hydrogen peroxide can be easily self-decomposed at the room temperature, the liquid container is immersed in an ice/water mixture to maintain its temperature of 0 °C, preventing the self-decomposition of the liquid hydrogen peroxide. A soft plastic capillary tube with its inner diameter of 1.0 mm is used to transfer the liquid from the container to the silicon chip. The capillary tube is observed to have the liquid filled without any gas bubbles inside, ensuring the liquid state of the hydrogen peroxide at the inlet of the silicon chip. A 2 μm filter is arranged in the capillary pipeline to prevent any solid particles entering the silicon chip. There is also a miniature on/off valve on the pipeline.

2.3. Instrumentation and measurement uncertainty

The pressure upstream of the silicon chip is measured by a Setra pressure transducer (model 206) with the accuracy of 1% and the response time of 0.2 s. The fluid temperatures of the inlet and outlet of the silicon chip are measured by the K-type jacket thermocouples with the uncertainty of 0.3 °C. The outlet liquid mass flow rate is determined by weighing the collected mass over a given period of time using a precision electronic balance with the uncertainty of 0.002 g. The oxygen gas produced by the chemical reaction is automatically escaped to the air environment.

The transient two-phase flow patterns with catalytic chemical reaction are observed by a high speed camera (HG-100 K, Readlake Inc. USA) combined with a Leica

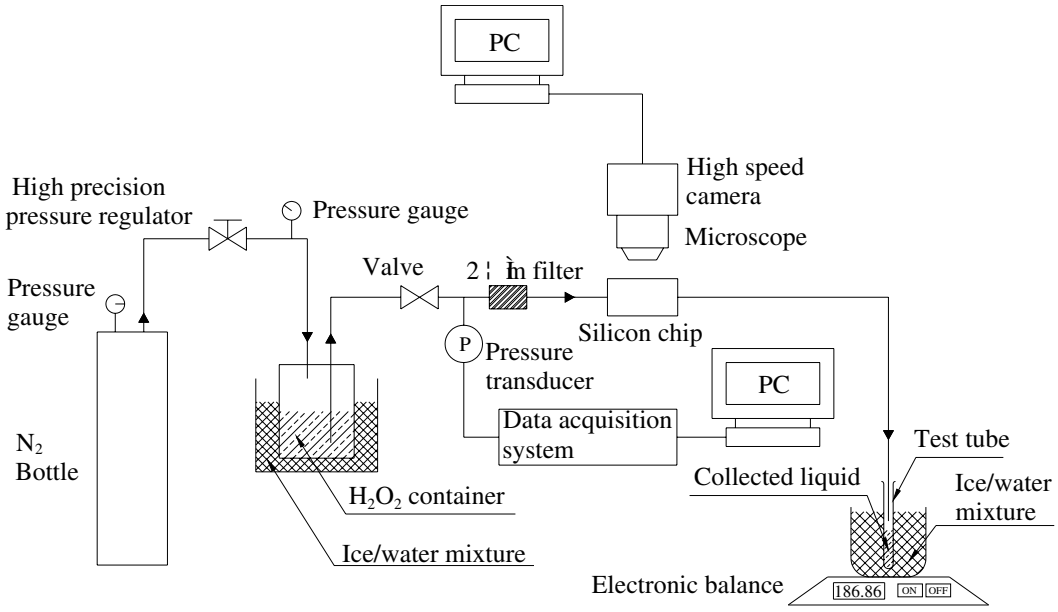

Fig. 3. Experimental setup and high speed flow visualization system for the transient two-phase flow with chemical reactions in the microreactor.

M stereo microscope (Germany) via an one inch port. A cold light source is turned on to form clear images on the PC screen. The maximum recording rate can be up to 5000 frames per second, with the resolution of 1504×1128 pixels. However, very high recording rate requires a very powerful light source. Depending on the response of the transient flow, the present experiment uses the recording rates of 500, 250 or 125 frames per second.

The one-dimensional coordinate system was attached on the centerline of each microchannel and starts from the microchannel entrance. The commercial software PHOTOSHOP 6 was used to process the captured images. Along the flow direction, one unit axial pixel scales the axial length of 8.86 μm, which is the length resolution of the flow visualization system. We count the axial pixel number which is focused on the center point of the selected liquid slug. Thus the liquid slug displacement can be obtained by converting the pixel number into the length unit. A selected bubble slug length can be obtained by converting the axial pixel number difference between the front and tail of the selected bubble slug into the length unit.

3. Data reduction

The above section describes the instrumentation and measurement uncertainties. These parameters are named as the "direct" measured parameters. The indirect parameters are the outlet mass concentration of hydrogen peroxide and the decomposition ratio, which need the titration and data reduction processes.

The liquid hydrogen peroxide (H_2O_2) can be self-decomposed into water or vapor (H_2O) and oxygen gas (O_2) on the catalyzed solid wall surface such as platinum according to the following equation:

$$H_2O_2\ (\text{liquid}) \rightarrow H_2O\ (\text{liquid}) + \frac{1}{2}O_2\ (\text{gas}) + 98.11\ \text{kJ/mol} \quad (1)$$

With the water latent heat of evaporation (h_{fg}) of 44 kJ/mol, specific heat of liquid water ($c_{pf,water}$) of 75.25 J/mol K, specific heat of water vapor ($c_{pv,water}$) of 25.6 J/mol K, and specific heat of oxygen (c_{pv,O_2}) of 21.4 J/mol K, the microreactor temperature can be estimated at the given inlet mass concentration and decomposition ratio of hydrogen peroxide with the adiabatic assumption. However, the chip has large surface area that is exposed in the environment relative to the etched reactor volume. Heat created by the catalytic chemical reaction (Eq. (1)) is dissipated into the environment. Thus the catalytic chemical reaction is taking place at the room temperature level, which is verified by the backside surface temperature measurement using an Infrared Radiator Image System (FLIR ThermalCAM SC3000) with the temperature resolution of 0.02 °C and the temperature uncertainty of 0.5 °C. The calibration of the IR image system is described in [14]. During the experiment, the room temperature is well controlled at 20 °C with the uncertainty of 1 °C by the air conditioning system.

In an attempt to quantify the level of decomposition via the catalytic chemical reaction, the outlet mixture was collected and analyzed to determine the outlet mass concentration of hydrogen peroxide. The exit liquid is the unreacted hydrogen peroxide and water. The produced oxygen gas was released into the environment automatically.

The titrate method was used to determine the outlet hydrogen peroxide concentration. The hydrogen peroxide (H_2O_2) can take place the chemical reaction with potassium permanganate ($KMnO_4$) in the vitriol solution (H_2SO_4) according to the following equation:

$$2KMnO_4 + 3H_2SO_4 + 5H_2O_2 = K_2SO_4 + 2MnSO_4 + 5O_2 + 8H_2O \quad (2)$$

The titrate process starts from the preparation of the sample liquid. A 0.2 g sample liquid with the accuracy of 0.002 g was fetched from the collected liquid and diluted to a specific volume with the deionized water. Fetching 25 ml of such diluted sample liquid to a conical beaker which initially contains 35 ml vitriol acid (H_2SO_4). The potassium permanganate ($KMnO_4$) solution is titrated into such beaker until pink color lasts for 30 s. The collected hydrogen peroxide concentration is calculated as

$$c_2 = V \times c \times 0.01701 \times 100/m_{sam} \quad (3)$$

where V is the consumed volume of the potassium permanganate solution, c is the concentration of the potassium permanganate solution with the unit of mol/L and m_{sam} is the sample liquid mass to be titrated.

Once the hydrogen peroxide concentrations at the upstream and downstream of the silicon chip are known, the decomposition ratio, which is defined as the percentage of the decomposed hydrogen peroxide mass divided by the total hydrogen peroxide mass, can be written as

$$\alpha = \frac{17(c_1 - c_2)}{(17 - 8c_2)c_1} \quad (4)$$

where c_1 and c_2 are the hydrogen peroxide concentration at the upstream and downstream of the silicon chip. It is noted that Eq. (3) is derived based on the mass balances of the chemical reaction equation of Eq. (2). Eq. (4) is derived based on that of Eq. (1). The uncertainty of the hydrogen peroxide concentration measurement is 1.0%. The error of the decomposition ratio α comes from c_1 and c_2. Performing the standard error analysis based on Eq. (4), α has the maximum uncertainty of 0.02% which is quite small.

It is noted that the present experiment was performed at the "cold state" with the chip directly exposed in the air environment. The hydrogen peroxide decomposition ratio is low and in the range of 3–5% in the present paper. Thermal insulation of the silicon chip and use the smaller ratio of the chip surface that is exposed in the environment to the etched substrate volume will greatly increase the chip temperature level. Under such condition the transient process evolves much faster and the hydrogen peroxide decomposition will be enhanced from the chemical reaction kinematic point of view.

4. Results and discussion

4.1. General description of the transient chemical reaction flow in microchannels

The chemical reaction flow was observed by the high speed camera incorporated with a microscope. There is a balance between the recording rate and the physical recording time. If a transient flow evolves fast with short cycle period, the recording rate should be high but the physical recording time is short. For the slow transient with short cycle period such as 1 s, the recording rate is set as 1000 or 500 frames per second. On the other hand, if the cycle period is long such as 6 s, the low recording rate of

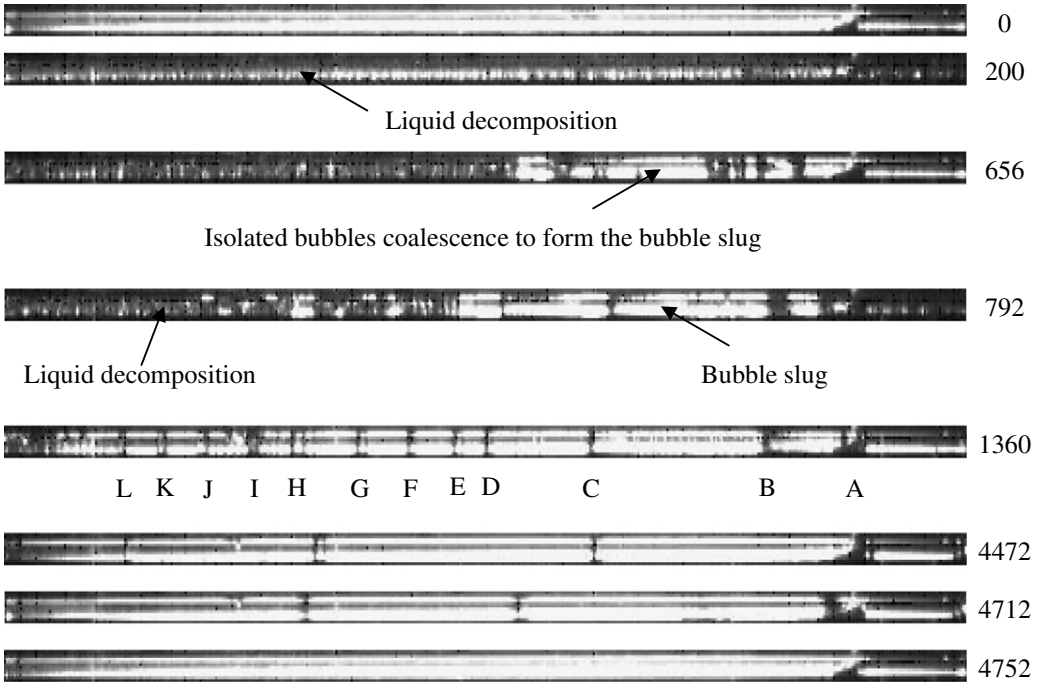

Fig. 4. Transient process for a full cycle based on microchannel 7 at 60% inlet mass concentration of hydrogen peroxide and 15 kPa pressure drop (the unit of time sequence is ms).

125 frames per second is used. Under either condition more than 1000 frames were captured for each run case. The flow view area covers the whole etched surface including the inlet liquid plenum, the nine parallel rectangular microchannels and the planar converging–diverging nozzle.

The transient hydrogen peroxide decomposition and two-phase flow display the strong cyclic behavior for each microchannel. Such cyclic behavior is not isochronous among different channels. Generally a full cycle can be divided into three substages: quick liquid refilling stage, liquid decomposition stage and bubble slug flow stage. A successive of images showing the complicated decomposition and two-phase flow are shown in Fig. 4 for the reservoir hydrogen peroxide concentration of 60% and the pressure drop of 15 kPa. A successive of images for a full cycle are demonstrated based on microchannel 7.

Liquid refilling stage ($0 < t < 200$ ms). The initial time ($t = 0$ ms) is defined as the time when the selected microchannel 7 is covered by the liquid (first image in Fig. 4, liquid refilling stage). Generally the liquid refilling stage lasts very short in the order of several milliseconds.

Catalytic decomposition stage (200 ms $< t <$ 1360 ms). At $t = 200$ ms the microchannel 7 becomes blurred, indicating the decomposition chemical reaction in such microchannel. At $t = 656$ ms the isolated bubbles in microchannel 7 begins to coalescence, forming the bubble slug in the downstream part of the microchannel. With time evolving several bubble slugs are formed. A liquid slug, indicated by the local black spot, exists between two neighboring bubble slugs. In other words, several liquid slugs separate the corresponding number of the bubble slugs. The maximum number of the liquid slugs takes place at $t = 1360$ ms. Thus the first critical time occurs at $t = 1360$ ms. A successive of liquid slugs are marked from A to L, in which the liquid slug A is close to the microchannel downstream while the liquid slug L is near the microchannel entrance. The twelve liquid slugs from A to L involve thirteen bubble slugs with the average bubble slug length of 0.46 mm in the microchannel 7. The formation of the maximum number of liquid slugs indicates the ending of the decomposition stage. As observed, the bubble slugs are not uniformly distributed in length, with shorter bubble slugs in the channel upstream and longer bubble slugs in the channel downstream.

Generally in the hydrogen peroxide decomposition stage the isolated bubbles produced by the catalytic chemical reaction and bubble slugs coexist in microchannels. The catalytic chemical reaction dominates the process. Such status sustains until a critical time is reached when the maximum liquid slugs are produced, separating the whole microchannel length into several parts with each corresponding to a bubble slug.

Bubble slug flow stage (1360 ms $< t <$ 4712 ms). The liquid and bubble slugs are moving slowly in this stage. At low reservoir hydrogen peroxide concentration such as the run case shown in Fig. 4, the fluid moves both

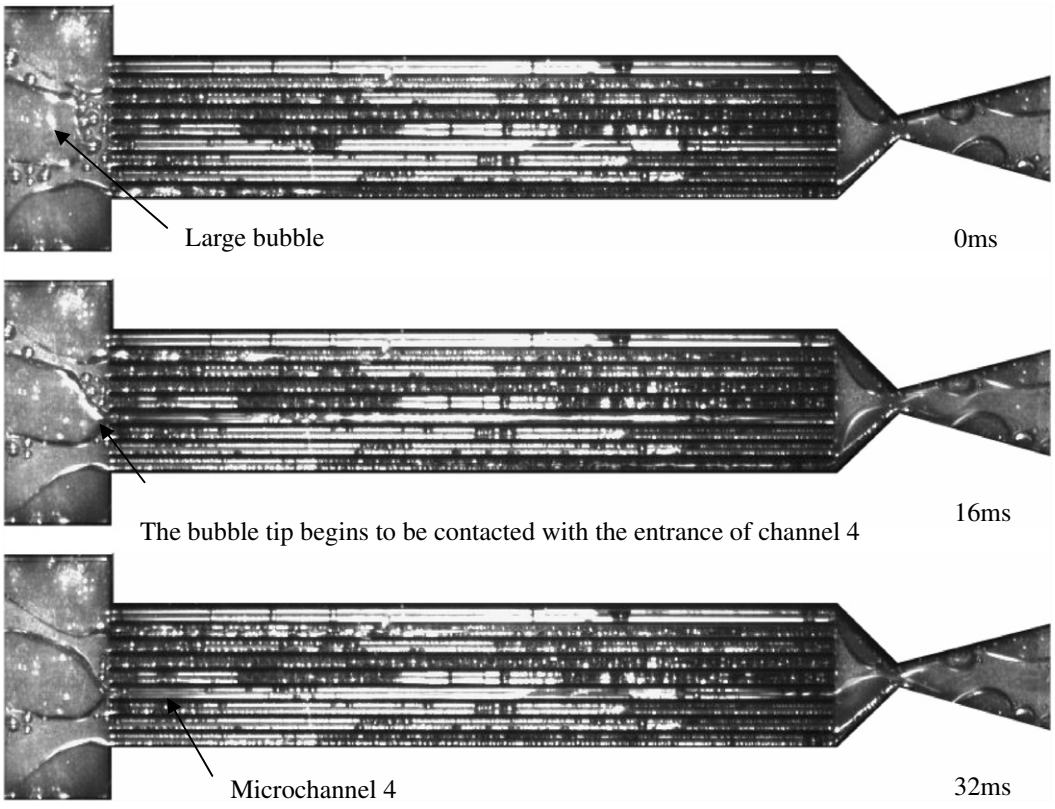

Fig. 5. The large bubbles populated in the inlet plenum of the silicon chip.

downstream and upstream (flow reversal phenomenon), which is caused by the following three factors: the upstream applied pressure, the increased pressure induced by the catalytic chemical reaction between the liquid film of hydrogen peroxide and the catalytic solid wall surface, and the liquid decomposition site distribution along the flow direction. At the same applied pressure, the lower mass concentration of the hydrogen peroxide results in the quasi-uniform liquid decomposition site distribution along the flow direction (see the image at $t = 200$ ms in Fig. 4). The simultaneous liquid decomposition in downstream of the microchannel yields the increased pressure there, resisting the upstream fluid moving downward, causing the fluid moving back to the inlet plenum of the silicon chip. However, we observed that the liquid decomposition mostly takes place in the microchannel upstream at the higher mass concentration of the hydrogen peroxide, causing the upstream fluid easily moving downstream of the microchannel. This is why we did not observe the flow reversal phenomenon at the high inlet mass concentration of the hydrogen peroxide.

Gradually, the slowly moving liquid slugs will arrive at the microchannel exit, leading to the decreased number of the liquid slugs in microchannels. Correspondingly the bubble slug lengths are increased, which are coming from the continuous catalytic chemical reaction between the liquid film surrounding the gas core of the bubble slug and the catalytic solid wall surface. Thus it is seen that the catalytic chemical reaction still takes place in this stage. This stage sustains until the second critical time is reached when the less number of liquid slugs begin to be quickly flushed out of microchannels, which occurs at $t =$ 4712 ms in Fig. 4. Once all the liquid slugs are out of microchannels then fresh hydrogen peroxide liquid refills the microchannel (see Fig. 4, the last image at $t = 4752$ ms). Then a new cycle starts.

4.2. Liquid decomposition and flow status in the inlet liquid plenum

In the present study, the hydrogen peroxide container is immersed in the ice/water mixture thus there is no any self-decomposition in the capillary tube connecting the liquid container and the silicon chip. However, there are two or three large bubbles observed in the inlet plenum of the microreactor, which are generated by the following two mechanisms. The first one is the reversed flow from the microchannel reactor to the inlet plenum of the silicon chip. The second is the self-decomposition of hydrogen peroxide in the inlet plenum. The reversed flow from the

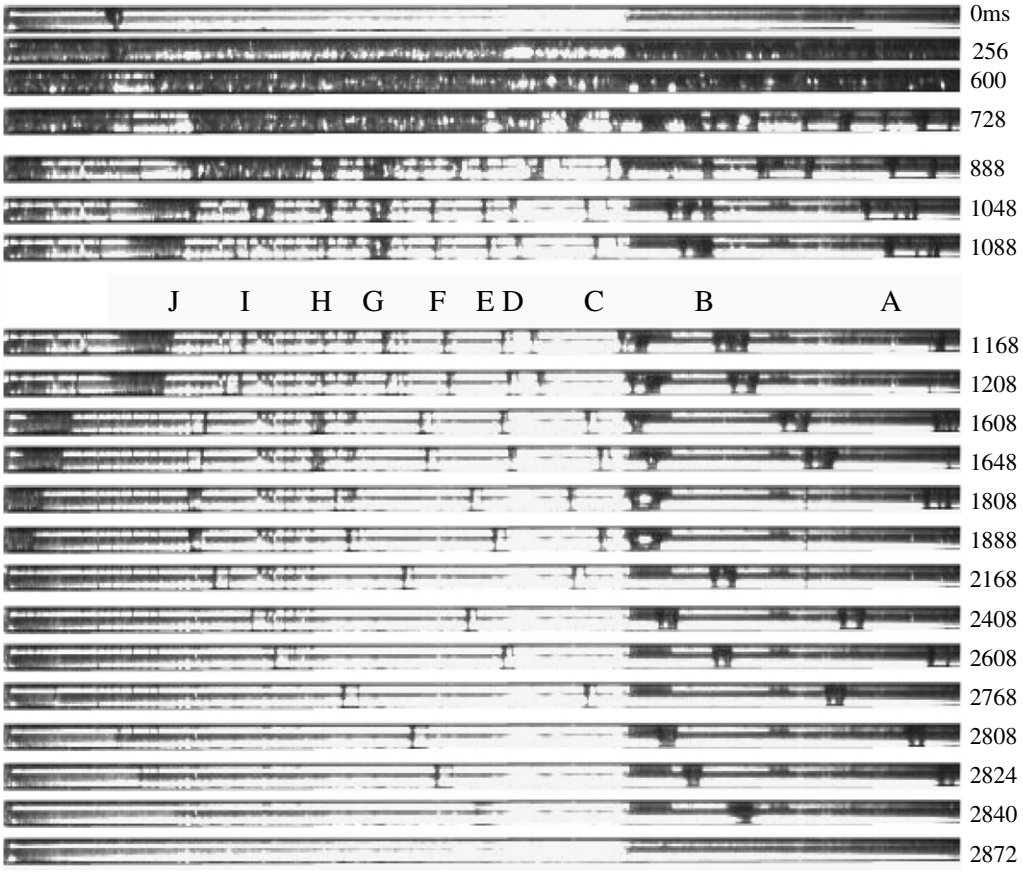

Fig. 6. Transient two-phase flow with chemical reactions in microchannel 9 at 60% inlet mass concentration of hydrogen peroxide and 15 kPa pressure drop (Fresh liquid refills the channel at $t = 0$, hydrogen peroxide decomposition for $104 < t < 1088$ ms, bubble slug flow for 1088 ms $< t <$ 2824 ms, the image at $t = 2840$ ms repeats the liquid refilling state, the unit of time is ms).

microchannel to the inlet plenum takes place not only in the present microchannel reactor, but also in some micro evaporators (heat exchangers) with boiling heat transfer inside the parallel microchannels [15,16,10]. It cannot be avoided under some circumstances.

The inherent MEMS fabrication technique cannot perform the selective deposition of the thin platinum film on the etched surface of the silicon chip, leading to the whole exposed etched surface (the side and bottom surfaces of the microchannels, the inlet plenum and the exit planar micronozzles), covered by the catalytic platinum film. There are two effects of the deposited platinum film in the inlet plenum. The positive effect is acted as the catalytic surface that contributes more catalytic surface area. The negative effect is to form the large bubble in the inlet plenum caused by the hydrogen peroxide self-decomposition, leading to the uneven flow among the multichannels.

No matter how the bubble is generated in the inlet plenum, it tends to be accumulated in the corner of the inlet plenum due to the surface tension effect (see Fig. 5). This effect causes the larger possibility that the entrance of the side channels, such as channels 1 and 9 are immersed in the gas phase. In other words, the side channels have fewer possibilities that are flushed by the hydrogen peroxide liquid. Instead, there are longer bubble slugs in the side channels with less liquid slugs inside.

Sometimes it is observed that the third bubble located in the center region of the inlet plenum (see Fig. 5). Compared with the corner bubbles in the inlet plenum, the center bubble in the inlet plenum is not stably populated but will be pushed to the microchannel again by the pressure-driven flow.

4.3. Liquid slug displacement and bubble slug length in microchannels

In the microchannel reactor, the isolated bubbles and bubble slugs are the two major flow patterns. The former one occurs in the hydrogen peroxide decomposition stage while the later one takes place in the bubble slug flow stage. The transition from the isolated bubbles to the bubble slug flow depends on the isolated bubble densities in microchannels. When the isolated bubble number is increased to a certain value, the bubbles coalescence to form the bubble slug due to the shortened distance of the isolated bubbles. Annular flow is an expected one with gas core in the channel center region and the thin liquid film attached on the catalytic wall surface. Such flow has no liquid droplet, providing large contact surface between the liquid and the catalytic solid wall, leading to the complete decomposition of hydrogen peroxide.

Figs. 6 and 7 show the two-phase flow with chemical reactions in microchannel 9 (side channel) and 7 respectively, for the inlet hydrogen peroxide mass concentration of 60% and pressure drop of 15 kPa. Because the transient process is not isochronous for different channels, the initial

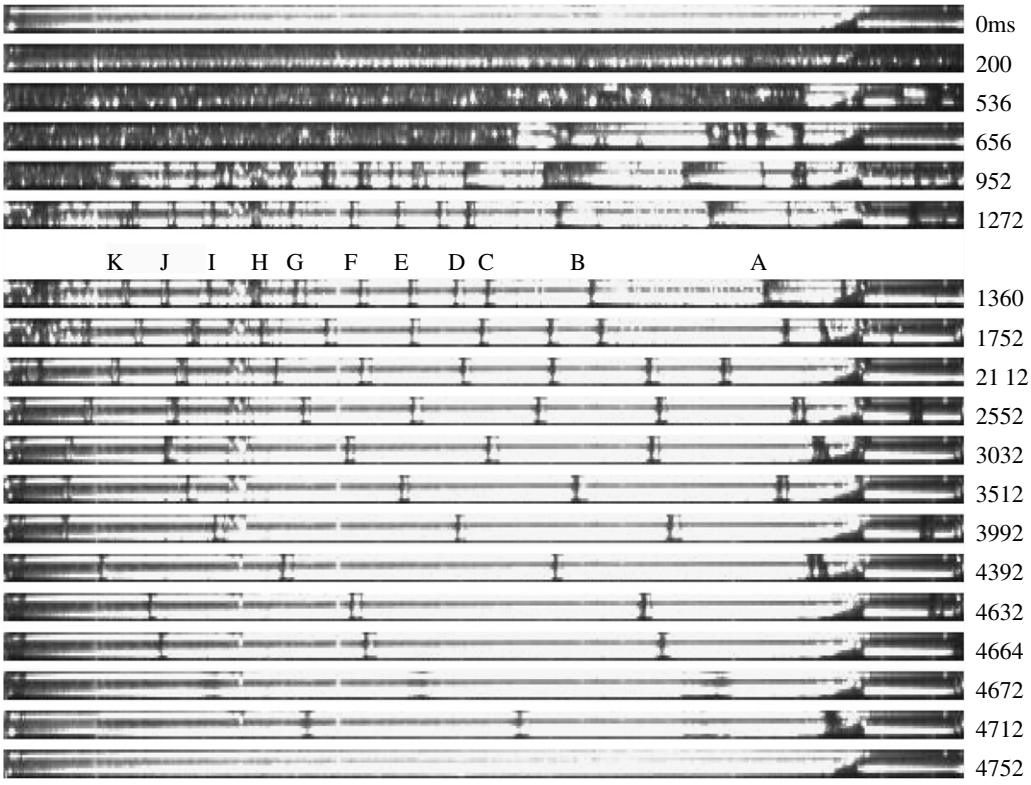

Fig. 7. Transient two-phase flow with chemical reactions in microchannel 7 at 60% inlet mass concentration of hydrogen peroxide and 15 kPa pressure drop (the unit of time sequence is ms).

time $t = 0$ is defined for each channel independently. In microchannel 9, the fresh liquid of hydrogen peroxide covers the whole channel at $t = 0$ (see Fig. 6). The whole microchannel evolves the hydrogen peroxide decomposition process, indicated by the blurred image from 256 ms to 600 ms. The isolated bubbles begin to coalescence, forming the bubble slugs in downstream part of the microchannel for the time of 728–1088 ms. The first critical time occurs at $t = 1088$ ms when there exists the maximum number of liquid slugs, separating a set of bubble slugs. Again the liquid slugs are marked from A to J at $t = 1088$ ms.

The bubble slug flow starts from 1088 ms. Putting a set of transient images together versus time, one can clearly identify the liquid slug trajectories. Flow reversal phenomenon was observed for liquid slugs J and I, indicated by the decreased liquid slug displacements versus time. Because the liquid slugs are continuously out of microchannels, for instance, the liquid slugs A, B and C disappear in the microchannel 9 at $t = 1208$ ms, $t = 1648$ ms and $t = 1888$ ms, respectively, the bubble slug lengths are increased corresponding to the decreased number of liquid slugs in the microchannel. The fluid is quickly flushed out of the microchannel around at 2824 ms (the second critical time). A new cycle begins with fresh liquid refilling the microchannel (see Fig. 6, $t = 2840$ ms). Similar transient process is shown in Fig. 7 for the center channel 7.

Fig. 8 illustrates the liquid slug displacements and bubble slug lengths for the case shown in Figs. 6 and 7. It is noted that the initial time $t = 0$ in Fig. 8 starts from the bubble slug flow stage, not including the hydrogen peroxide decomposition process. $t = 0$ is also the first critical state at which there are the maximum number of liquid slugs. The second critical time is marked as t_a at which three liquid slugs existed in channels. The steep gradients of the liquid slug displacements following the second critical time indicate the fast moving speed of the liquids. One may expect the average traveling speeds of the liquid slugs. Such values are computed as 3.37 mm/s and 2.85 mm/s for the liquid slugs B and C, respectively, for the side microchannel 9, based on Fig. 8. The reversal flow velocity is estimated as 0.99 mm/s for the liquid slug J which is traveling upstream of the microchannel. For the microchannel 7, the traveling speeds are 3.09 mm/s, 2.30 mm/s, and −0.475 mm/s for the liquid slugs B, C and K, respectively, in which the negative speed indicates the reversal flow for the liquid slug K.

Fig. 9 shows a set of chemical reaction and two-phase flow images for the microchannel 5 while Fig. 10 is for the liquid slug displacements and bubble slug length distributions at high inlet mass concentration of hydrogen peroxide of 90%. From Figs. 8 and 10, it is seen that the flow reversal takes place at low mass concentration of 60%, which can be

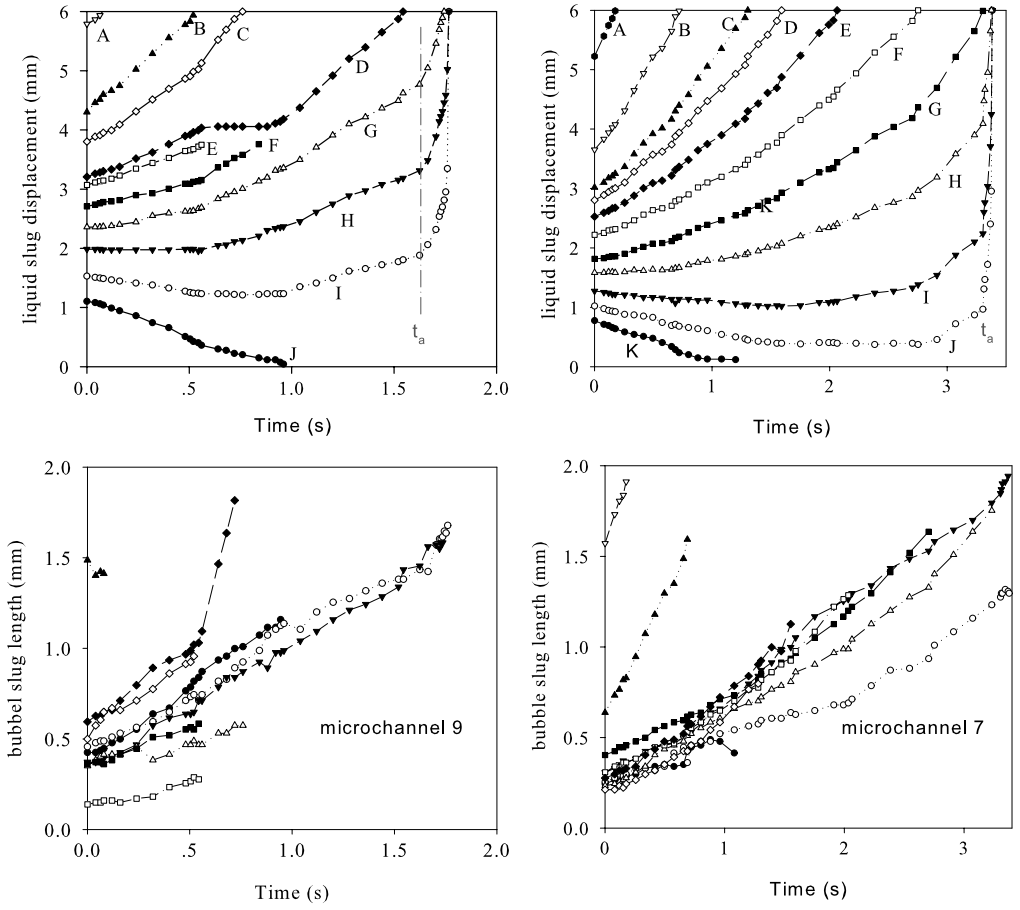

Fig. 8. Liquid slug displacement and bubble slug length versus time for 60% inlet mass concentration of hydrogen peroxide and 15 kPa pressure drop.

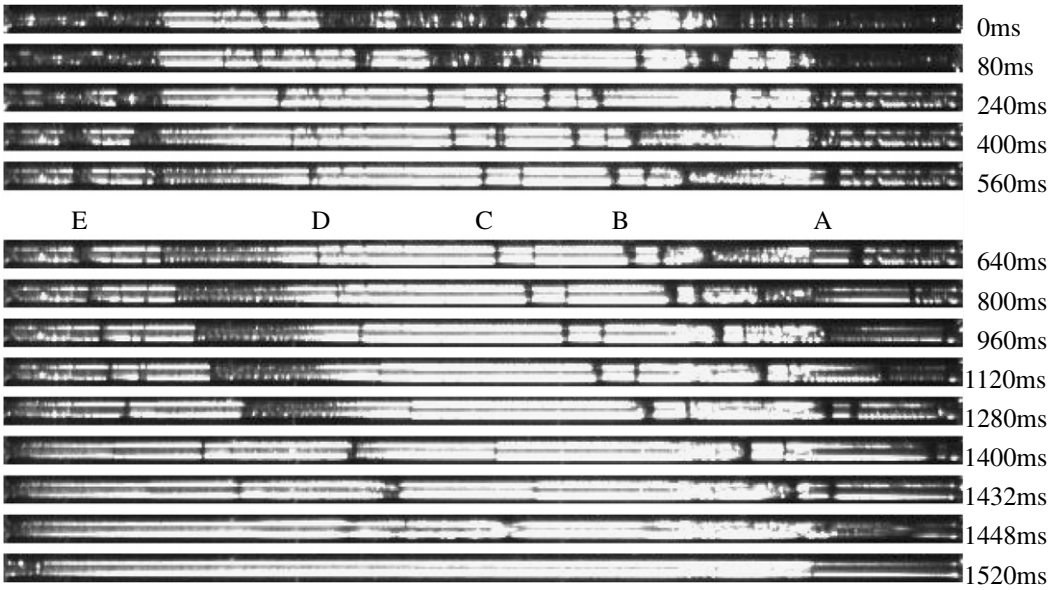

Fig. 9. Transient two-phase flow with chemical reactions in microchannel 5 at 90% inlet mass concentration of hydrogen peroxide and 15 kPa pressure drop.

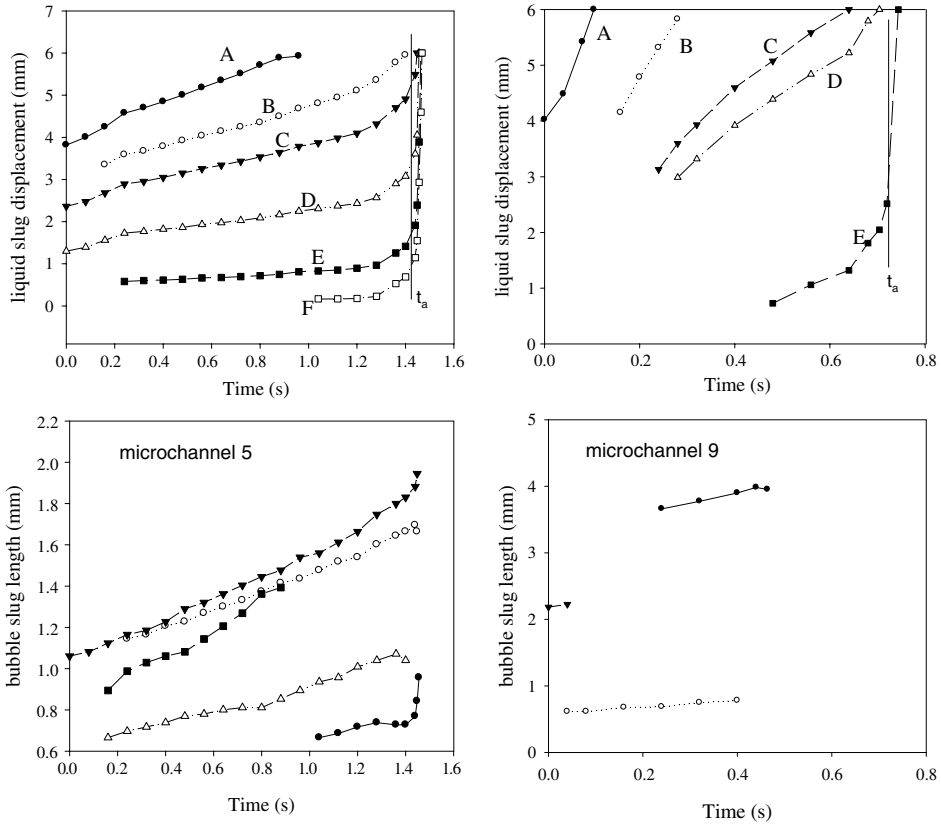

Fig. 10. Liquid slug displacement and bubble slug length in microchannels 5 and 9 at 90% inlet mass concentration of hydrogen peroxide and 15 kPa pressure drop.

easily identified by the decreased liquid slug displacements, such as I, J for the side channel 9 and I, J and K for the center channel 7 (see Fig. 8). The flow reversal is not observed for the high inlet mass concentration of 90% in Fig. 10. This is because the lower inlet mass concentration of hydrogen peroxide causes the uniform liquid decomposition along the axial flow direction. The liquid decomposition at the downstream of the microchannels resists the

upstream fluid traveling downward thus the flow reversal occurs. On the other hand, the higher inlet mass concentration of hydrogen peroxide enhances the liquid decomposition at the channel upstream but weakens the liquid decomposition at the channel downstream, causing the upstream fluid easily traveling downward.

The initial bubble slug lengths are around 0.5 mm for the side channel 9, which is longer than 0.3 mm for the center channel 7 at low inlet mass concentration of 60% (see Fig. 8). On the other hand, they are in the range of 0.8–4.0 mm and 0.6–1.0 mm for the side channel 9 and center channel 5 respectively at high inlet mass concentration of 90% (see Fig. 10). Thus it is seen that the initial bubble slug lengths are longer for the side channels than those for the center channels at both low and high inlet mass concentrations. As seen from Fig. 5, there are two corner bubbles stably populated in the two corners of the inlet plenum. The entrance of the side channel 9 has the largest possibility that is covered by the gas phase and smallest possibility that is flushed by the liquid. Thus there is less liquid slug number and the bubble slug length is longer in the side channel.

The quasi-linear distributions of liquid slug displacements and bubble slug lengths versus time are observed before the second critical time is reached for both low and high inlet mass concentrations. The liquid slugs in microchannels are responsible for the incomplete liquid decomposition. Seeing from a successive of images in Figs. 6 and 7 is that the liquid slug sizes (indicated by a set of local black spots) do not change versus time. This is because the liquid slugs have less contact surface area with the catalytic solid wall surface. The unreacted liquid slugs will be directly expelled out of the silicon chip at the end of each cycle. A rough estimate of the total volume of liquid slugs $A, B, \ldots, J$ is $2.8 \times 10^{-6}\,\mathrm{cm}^3$ in Fig. 6, corresponding to the liquid mass of 2.8 μg assuming the liquid density of $1000\,\mathrm{kg/m}^3$. Meanwhile the total bubble slugs have the volume of 54.8×10^{-6} ml, corresponding to the gas mass of 0.071 μg produced by the catalytic chemical reaction with the oxygen gas density of $1.295\,\mathrm{kg/m}^3$ at the atmosphere pressure and room temperature. Thus it is seen that the unreacted hydrogen peroxide mass is quite large than the reacted hydrogen peroxide mass, even though the gas phase from the reacted hydrogen peroxide covers the dominant microchannel volume. The above simple estimation gives the decomposition ratio of 2.5%, which roughly matches the decomposition ratio of 3.1% given by the hydrogen peroxide titrate process.

The initial bubble slug lengths reported in Figs. 8 and 10 are important for the future microreactor design. In any case they are much shorter than the critical length of 1.7–2.0 mm given by Hitt [4]. One would expect the annular flow in microchannels if the microreactor length is less than the bubble slug lengths in Figs. 8 and 10. Under such condition there are no liquid slugs, greatly enhancing the decomposition ratio of the hydrogen peroxide. It is noted that such extension should take account of the temperature effect, which is recommended for the future studies.

Now we turn to give a simple analysis of the traveling speed of the liquid slugs. Because the constant pressure is powered by the nitrogen gas, different pressure drops are sustained for each liquid slug when the number of liquid slugs is changed. Before the second critical time t_a is reached, the number of liquid slugs is large, leading to smaller pressure drop across each liquid slug sustained. However, once a specific time such as t_a is reached, there are less liquid slugs in microchannels, leading to a higher pressure drop across each liquid slug sustained. Thus the liquid slugs are accelerated and flushed out of microchannels quickly following such critical time.

4.4. Cycle behavior and mass flow rate of the transient chemical reaction flow

The statistic analysis of the cycle periods was performed to identify the effects of the inlet mass concentrations of hydrogen peroxide, pressure drops and multichannels.

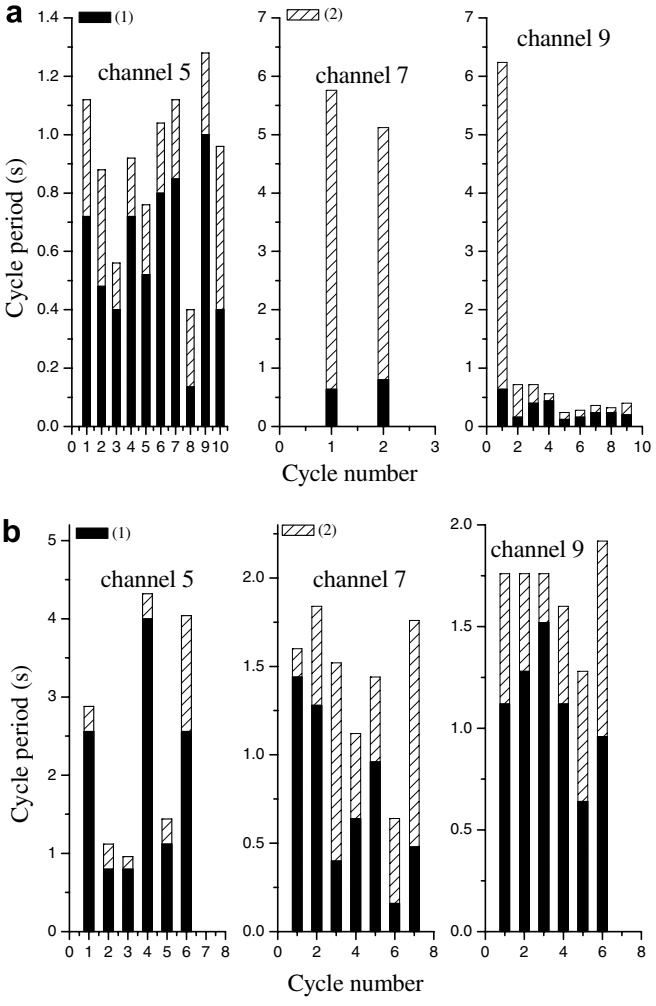

Fig. 11. Effect of inlet mass concentrations of hydrogen peroxide on the cycle periods (a) 50% inlet mass concentration of hydrogen peroxide and 15 kPa pressure drop, (b) 90% inlet mass concentration of hydrogen peroxide and 15 kPa pressure drop. (1) liquid decomposition stage, (2) bubble slug flow stage.

The cycle periods are plotted versus a successive of cycle numbers in Fig. 11 for microchannels 5 (the center channel), 7 and 9 (the side channel), respectively. The fresh liquid refilling stage only covers several milliseconds, thus it is neglected. The black pillar indicates the time of hydrogen peroxide decomposition stage while the other part indicates the time of bubble slug flow stage. It is seen from Fig. 11 that the cycle periods are not constant for a successive of cycle numbers, but they are oscillating against the average values and satisfy the statistic principle for a specific channel. For instance, for the run case of inlet mass concentration of hydrogen peroxide of 50% and pressure drop of 15 kPa (see Fig. 11a), the statistic analysis for the successive of ten cycles demonstrate that the average cycle period is 0.904 s, with the deviation of 0.255 s for the microchannel 5 (the center channel). The general trend of the average cycle periods for different channels is that the center channel has shorter cycle periods while the side channels possess the longer values. The oxygen gas–liquid flow produced by the catalytic chemical reaction is similar to the boiling flow in microchannels. When the hydrogen peroxide liquid is flushed in the microchannel, we do not know the exact locations of the local catalytic wall surface that triggers the catalytic chemical reactions. The active "nucleation sites" are randomly distributed on the wall surface, but the optimal shapes and sizes of the active

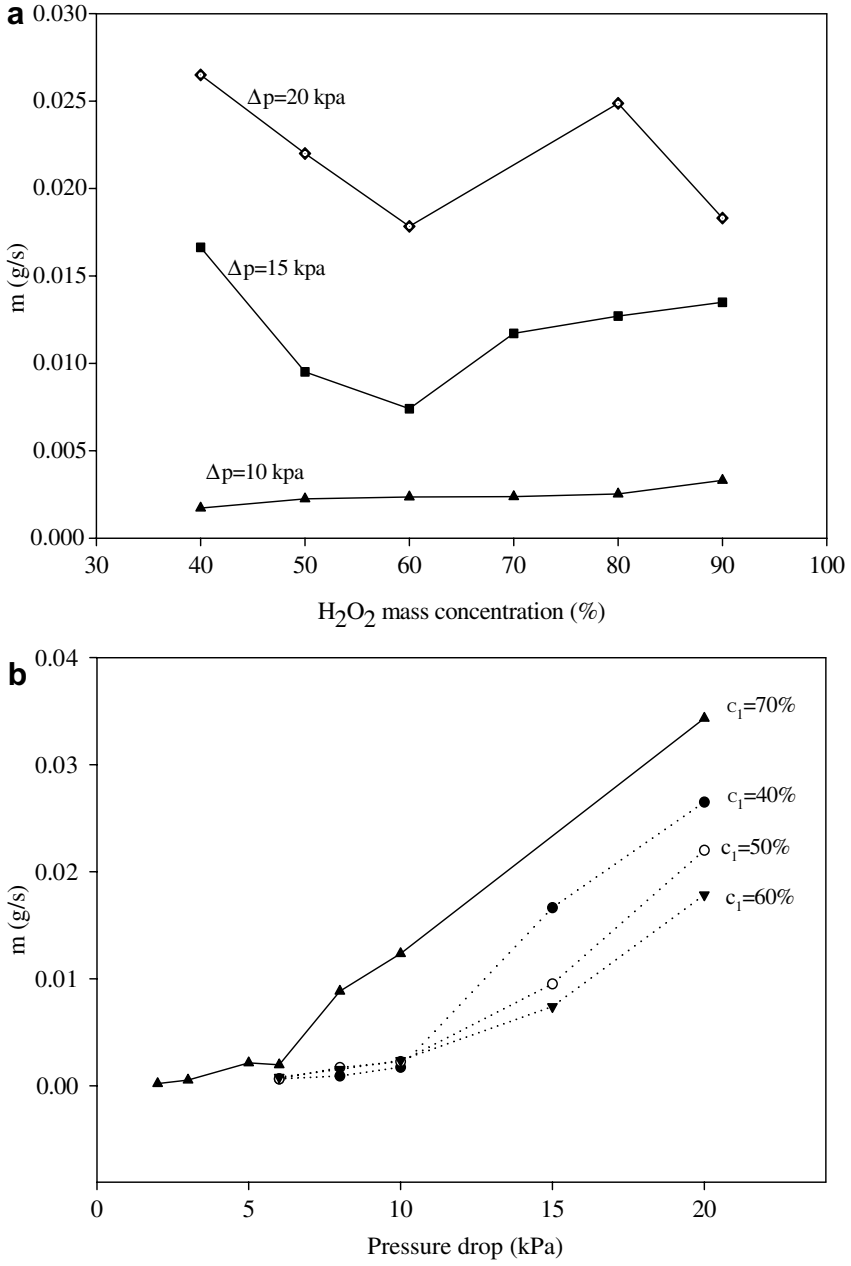

Fig. 12. Effect of hydrogen peroxide concentration and pressure drop on mass flow rate.

"nucleation site" satisfy the statistic principle, which finally yield the statistic distribution of the cycle periods. This analysis also partially explains the in-synchronous behavior of the chemical reaction flows among different channels.

It is interesting to note that the catalytic chemical reaction time is around 1 s for different cycle numbers and channels at 60% hydrogen peroxide concentration. The higher pressure drop greatly decreases the relative time of the bubble slug flow over the total cycle periods, due to the fact that higher pressure drop applied on each single liquid slug can easily pushes the liquid slugs out of microchannels.

By comparing the two subfigures of Fig. 11, the hydrogen peroxide decomposition takes the time in the range of 0.4–1.0 s for 50% inlet mass concentration while it takes longer time for the 90% inlet mass concentration. From the catalytic chemical reaction point of view, the reaction time is dependent on the initial mass concentration of the hydrogen peroxide, the temperature level and the liquid mass that is to be reacted. For the similar temperature environment, one expects an intensive chemical reaction thus a short decomposition time is needed with the higher initial mass concentration of hydrogen peroxide. However, the higher mass concentration of 90% provides nearly two times of the pure hydrogen peroxide mass that is to be decomposed than the lower initial mass concentration of 50%. This effect causes the longer decomposition time for the 90% mass concentration of hydrogen peroxide.

Finally, we demonstrate the measured mass flow rates dependent on the inlet hydrogen peroxide mass concentrations and pressure drops in Fig. 12. It is seen from Fig. 12a that the mass flow rates are decreased and attain the minimum value with continuous increasing the inlet hydrogen peroxide concentrations at higher pressure drops such as 15 kPa and 20 kPa. Further increase the hydrogen peroxide concentration beyond the minimum point will increase the mass flow rates. It is well known that the two-phase pressure drop is dependent on the mass flow rate and the gas mass quality. Inversely, the mass flow rate through the microreactor is relied on the pressure drop and the gas mass quality. At the fixed pressure drop, increasing the inlet mass concentration of hydrogen peroxide yields the increased gas mass quality produced by the catalytic chemical reactions, leading to the decreased mass flow rate through the microreactor. This is true once the fluid residence time is less than the critical value. Once the fluid residence time is beyond the critical value, further increasing the inlet mass concentration of hydrogen peroxide yields the less gas mass produced in microchannels, leading to the increased mass flow rate of hydrogen peroxide. In other words, higher inlet mass concentration such as larger than 60% causes more hydrogen peroxide going out of the microchannels without fully catalytic chemical reactions. This effect deduces the increased mass flow rate through microchannels with increasing the inlet mass concentration of hydrogen peroxide after it is larger than 60%.

5. Conclusions

The present study identifies the transient two-phase flow with chemical reactions in a microchannel reactor. The following conclusions can be drawn:

- The transient two-phase flow with chemical reactions displays the strong cyclic behavior. A full cycle can be divided into three stages: the quick fresh liquid refilling stage, the liquid decomposition stage and the bubble slug flow stage.
- The liquid refilling stage covers very short time in the order of millisecond. In the liquid decomposition stage, the isolated bubbles and the bubble slugs coexist in microchannels. This stage ends at the first critical time when the number of liquid slugs in microchannels is maximum.
- In the bubble slug flow stage, a successive of liquid slugs separate the whole microchannel length into a set of bubble slugs. With time evolving, liquid slugs are gradually moving out of microchannels, leading to the increased bubble slug length. The bubble slug flow stage sustains until the second critical time is reached at which less liquid slugs exist in microchannels. Following such specific time, the fluid will be flushed out of microchannels quickly.
- The initial formed bubble slug lengths are useful for the optimized microreactor design. If one uses the microchannel length less than the initial formed bubble slug length, annular flow will be expected without liquid droplet formation to perform the complete liquid decomposition. The initial bubble slug lengths reported in the present paper are shorter than that given in Ref. [4]. Further study on the effect of chip temperatures on the bubble slug lengths is expected.
- The cycle behavior is not isochronous among different microchannels. The cycle periods satisfy the statistical principle even though they are oscillating for a successive of cycle numbers and channels.

Acknowledgements

This work is supported by the National Natural Science Foundation of China (50476088), the International Cooperation Project Funding from Chinese Academy of Science (GJHZ05) and Natural Science Foundation of Guangdong Province (5000729).

References

[1] R.L. Bayt, A.A. Ayon, K.S. Breuer, A performance evaluation of MEMS-based micronozzles, in: AIAA Proc. 33rd AIAA/ASME/ASEE Joint Propulsion Conf. Exhibit, Seattle, WA, USA, 1997, pp. 97–3169.

[2] K.L. Zhang, S.K. Chou, S.S. Ang, MEMS-based solid propellant microthruster design, simulation, fabrication and testing, J. Microelectromech. Syst. 13 (2) (2004) 165–175.

[3] D.K. Maurya, S. Das, S.K. Lahiri, Silicon MEMS vaporizing liquid microthruster with internal microheater, J. Micromech. Microeng. 15 (2005) 966–970.
[4] D.L. Hitt, C.M. Zakrzwski, M.A. Thomas, MEMS-based satellite micropropulsion via catalyzed hydrogen peroxide decomposition, Smart Mater. Struct. 10 (2001) 1163–1175.
[5] M. Kawajim, P.M.Y. Chung, Adiabatic gas–liquid flow in microchannels, Microscale Thermophys. Eng. 8 (3) (2004) 239–257.
[6] W.L. Qu, S.M. Yoon, I. Mudawar, Two-phase flow and heat transfer in rectangular microchannels, J. Electron. Pack. 126 (3) (2004) 288–300.
[7] R. Yun, Y. Kim, Flow regimes for horizontal two-phase flow of CO_2 in a heated narrow rectangular channel, Int. J. Multiphase Flow 30 (10) (2004) 1259–1270.
[8] P. Satichaicharoen, S. Wongwises, Two-phase flow pattern maps for vertical upward gas–liquid flow in mini-gap channels, Int. J. Multiphase Flow 30 (2) (2004) 225–236.
[9] H.Y. Wu, P. Cheng, Liquid/two-phase alternating flow during boiling in microchannels at high heat flux, Int. Commun. Heat Mass Transfer 30 (3) (2003) 295–302.
[10] J.L. Xu, Y.H. Gan, D.C. Zhang, X.H. Li, Microscale boiling heat transfer in a micro-timescale at high heat fluxes, J. Micromech. Microeng. 15 (2005) 362–376.
[11] B.R. Fu, C. Pan, Flow pattern transition instability in a microchannel with CO_2 bubbles produced by chemical reactions, Int. J. Heat Mass Transfer 48 (21–22) (2005) 4397–4409.
[12] T. Bewer, T. Beckmann, H. Dohle, J. Mergel, D. Stolten, Novel method for investigation of two-phase flow in liquid feed direct methanol fuel cells using an aqueous H_2O_2 solution, J. Power Sources 125 (1) (2004) 1–9.
[13] Y.H. Choi, S.U. Son, S.S. Lee, A micropump operating with chemically produced oxygen gas, Sens. Actuators, A 111 (2004) 8–13.
[14] J.L. Xu, Y.H. Gan, D.C. Zhang, X.H. Li, Microscale heat transfer enhancement using thermal boundary layer redeveloping concept, Int. J. Heat Mass Transfer 48 (2005) 1662–1674.
[15] S.G. Kandlikar, Fundamental issues related to flow boiling in minichannels and micro channels, Exp. Therm. Fluid Sci. 26 (2002) 389–407.
[16] S.G. Kandlikar, Heat transfer mechanisms during flow boiling in microchannels, ASME, J. Heat Transfer 126 (2004) 8–16.